J. Appl. Comput. Mech., 7(2) (2021) 611-620
DOI: 10.22055/JACM.2020.34893.2524

ISSN: 2383-4536
jacm.scu.ac.ir

Shahid Chamran University of Ahvaz

Journal of Applied and Computational Mechanics

Research Paper

Experimental and Numerical Investigation of Heat and Mass Transfer Processes for Determining the Optimal Design of an Accumulator with Phase Transformations

Ievgen Antypov, Valery Gorobets, Viktor Trokhaniak

Department of Heat and Power Engineering, National University of Life and Environmental Sciences of Ukraine
Heroyiv Oborony st., 15, Kyiv, 03041, Ukraine, Emails: ievgeniy_antypov@ukr.net, gorobetsv@ukr.net, trohaniak.v@gmail.com

Received September 09 2020; Revised November 26 2020; Accepted for publication November 28 2020.
Corresponding author: V. Trokhaniak (trohaniak.v@gmail.com)

Abstract. Applying the methods of mathematical and experimental modeling, the processes of heat and mass transfer in heat accumulator with phase transformations, where heat sources are made in the form of tube bundles staggered have been studied. The analysis of these processes is carried out and the main phases of heat accumulation and extraction at heat accumulator "charging" and "discharging" have been determined. The geometry of the location of heat sources (runoffs) is found, at which the rate of heat accumulation (extraction) from the unit of PCM is the maximum. As a result of the conducted investigations a new improved design of heat accumulator, which can be used when developing heat accumulators of a similar type has been suggested.

Keywords: Phase transformations, latent heat accumulator, numerical modeling, convective heat flux, optimal distance between heat sources.

1. Introduction

One of the promising areas of the development of energy supply of various facilities is the possibility to create energy self-sufficient complexes and own heating systems based on both traditional and renewable energy sources. However, it is known that the use of energy from these sources is complicated because of stochastic and uneven nature of heat accumulation in time during the day. As a result, there is a necessity to provide uninterrupted operation of these systems. Operational stability and reliability of such combined systems can be provided by both integrating traditional power supply sources into them and applying various types of energy accumulators. The analysis of various methods of heat accumulation has shown that the most promising type of heat accumulators is a heat accumulator with phase or chemical transformations of an accumulating material [1, 2]. Such accumulators provide high density of the accumulated energy in a mass unit of a heat-accumulating material and make it possible to maintain stabilized accumulator-exit temperature.

A number of publications [1-4] reviewed the existing heat storage materials used in heat accumulators with phase transformations and consider the scope of their application in the heat accumulation from different heat sources. An overview of heat storage materials with phase transformation temperatures in the range from 0 to 250 ° C and an assessment of the practical designs of heat exchange units for heat storage was presented by Pereira and Eames [3]. The studied materials can be used in heat accumulators at different coolant temperatures with accumulated heat from different types of sources. Kenisarin [4] summarized the results of previous studies of transition temperatures, melting point, heat capacity and thermal conductivity, long-term characteristics of many organic substances, their composition and compounds. Sharma *et al* [1] covered an overview of current research and storage of heat energy in phase storage heat accumulators, which are widely used in latent heat storage systems for heat pumps, solar technology and spacecraft thermal control programs, for heating and cooling buildings. Du *et al* [2] provided a state-of-the-art review of phase-change materials (PCMs) and their applications for heating, cooling and power generation according to the operating temperature range (-20 ° C to +200 ° C). The review showed that energy savings of up to 12% and a reduction in cooling load of up to 80% can be achieved with PCM in the low and medium low temperature range. PCM storage for heating systems can increase efficiency from 26% to 66%.

Pereira *et al* [5] studied the geometry and configuration of heat accumulations with a phase transition and conducted numerical and experimental studies to assess the impact of parameters such as inlet temperature and mass flow rate. It was indicated that the most suitable storage materials are those with a melting point in the range from 0 °C to 60 °C.

A number of the research [6-10] were devoted to the study of heat accumulation processes during phase transformations of PCM in capsule-type batteries. Suganya et al, Agyenim et al, Kalaiselvam *et al* [6, 7, 8] covered the analysis of the melting processes of paraffin, which is placed in cylindrical capsules used in the system of accumulation of heat energy from solar collectors. As a result of the conducted researches it was concluded that in accumulators of this type the thermal conductivity of PCMs has a

Published online: November 29 2020

dominant influence on the heat accumulation processes. The review by Sharma *et al* [9] focused on three aspects: materials, encapsulation, and the use of organic PCM, and provided an insight into recent developments in the use of these materials. Organic PCMs have low thermal conductivity (0.15-0.35 W/m K), and therefore, to increase the heat transfer rate requires a larger surface area. Therefore, attention was also paid to increasing the thermal conductivity of materials, which helps to minimize the surface area of the system. Organic PCMs are widely used in buildings and other areas of the use of solar energy with low and medium melting point. Trivedi and Parameshwaran [10] reviewed the technologies of heat accumulation in microcapsules during the phase transformation of the material. Demonstration projects and systems that use this technology were presented.

Huo and Rao [11] presented the results of experimental studies in a cylindrical capsule filled with PCM of phase transformation. The nature of the melting front during phase transformation was studied and the time required for complete phase transformation of three types of paraffin was determined: 60% n-tetradecane + 40% n-hexadecane, n-tetradecane and n-pentadecane. It was found that the total curing time depends on the Stefan number, and the total melting time depends on the equivalent thermal conductivity of PCM.

Wang *et al* [12] investigated the effect of emulsifier content on the structure and thermal properties of encapsulated paraffin materials during heat accumulation in capsules. These results showed that the piercing-solidifying method can be used for the manufacture of four kinds of paraffin/chitosan (CS) macro encapsulated PCMs with different emulsifier contents macro capsules with high heat storage and good thermal stability, but also reveal that paraffin/CS can be used at low temperature of PCM.

Lichołai *et al* [13] presented a study of heat transfer in blocks with paraffin pieces and composite windows depending on environmental conditions. The influence of geometric block sizes and PCMs volume values on environmental energy storage processes has been studied.

An important factor influencing the rate of heat accumulation is the thermal conductivity coefficient of PCM. Liu *et al* [14] presented an overview of experimental and numerical studies in order to improve the thermal conductivity of materials used in heat accumulators with phase transformations. Regin *et al* [15] covered methods for increasing the rate of phase change and the amount of latent accumulated heat per unit mass by improving the thermal conductivity of storage materials.

In the works [16-19] researches at use of the flat and finned surfaces for heat accumulation and extraction from PCM were carried out. Zhang *et al* [16] investigated the influence of the location of the heated wall on the paraffin melting process by numerical methods. The results showed that the location of the heating wall had great effects on the melting process. The paraffin in the cavity melted most quickly when the heating wall located at the bottom. After performing numerical simulations using MATLAB Simulink R2015b software based on the enthalpy method and ANSYS Fluent 15.0 Jegadheeswaran and Pohekar [17] investigated the influence of finned surfaces of different geometries on the efficiency of heat extraction processes in heat accumulators. It was shown that the use of finned surfaces increases the heat removal rate and reduces the "discharge" time of heat accumulator. Gorobets *et al* [18] presented the results of experimental studies of paraffin melting around a smooth and finned cylindrical heat source, including studies of the dynamic motion of the solid-liquid interface. The dependences of Nusselt number on the Rayleigh number for the intensive melting phase were obtained. In the experimental study of Arshad *et al* [20] the main attention was paid to passive cooling of electronic devices by means of heat dissipation based on phase material (paraffin), which fills finned radiators made of aluminum. The geometrical characteristics of the finned surface at which heat dissipation from electronic devices will be maximal were determined.

In the works of Kuboth *et al*, Mohamad *et al*, Karimnejad *et al* [20, 21, 22] the processes of heat accumulation during the phase transformations of heat-storing materials were investigated by numerical simulations using the Boltzmann lattice method. The application of this method allows to investigate in more detail the processes of melting and solidification of PCM, especially if a combined PCM with the addition of metal nanoparticles is used.

In some articles [23, 24] the thermophysical properties and influence of metal nanoparticles on the processes of heat accumulation in PCM were studied. Antypov *et al* [23] studied the effect of metal nanoparticles on the processes of heat accumulation in paraffin materials. It was shown that the presence of nanoparticles improves the heat accumulation rate in the phase transformation material by 20%. Nasieka *et al* [24] applied the methods of micro-Raman and photo- luminescent spectroscopy to determine thermo-physical properties of phase-transition materials with metal nanoparticles.

Some studies [25-27] were devoted to the study of heat and mass transfer processes in heat accumulators, where coils or pipe bundles were used as heat sources (drains). In the work written by Tpr [25] the latent thermal energy storage system of the shell-and-tube type during charging and discharging has been analyzed. A series of numerical calculations under different operating conditions of the coolant and different geometric parameters to increase system performance and optimize the design of the heat accumulator was performed. Naumov *et al* [26] proposed to use in containers for heat storage pipes with heat carrier, which have the shape of a coil and a metal mesh to intensify the heat transfer processes from heat sources. Gorobets *et al* [27] using numerical and experimental methods investigated the processes of heat accumulation in a container with paraffin at the staggered arrangement of cylindrical heat sources. The efficiency of this design of heat accumulators during heat accumulation from solar collectors, heat pumps and other renewable heat sources was shown.

It should be emphasized that the present scientific investigations do not pay enough attention to studying the processes that take place in heat accumulators with phase transformations, where tube bundles are the heat sources in the process of heat accumulation from solar collectors, heat pumps and other renewable sources.

This investigation is aimed at numerical and experimental investigation of the processes of heat and mass transfer at phase transformations of an accumulating material with low melting temperatures around several cylindrical heat sources and the development of the improved design of heat accumulators of this type.

2. Materials and Methods

Having analyzed the known designs of heat accumulators [26-29], a 2ew axonometric model (Fig.1) of the design of a heat accumulator with phase transformations has been suggested and developed using COMSOL Multiphysics 3.5a package [23, 27].

In the suggested design a cooling liquid comes into an accumulator and moves along the system of heating tubes arranged in a staggered order giving up or absorbing heat energy from an accumulating material. Paraffin T3 with its phase transformation temperature being T_f = 54÷56 °C was chosen to be a phase-change material.

When conducting numerical modeling of these processes, it was assumed that: 1) the body of a heat accumulator is thermally-insulated and there is no external heat loss; 2) the initial temperature is the same in the whole volume of an accumulating material; 3) the temperature of cylindrical heat source surfaces is determined from the heat balance between the heat that PCM obtains and the heat that is transferred to the material from a heat source. At the shear point of phase immiscibility, the heat that was absorbed (given up) during accumulating material melting (crystallization) was taken into account.

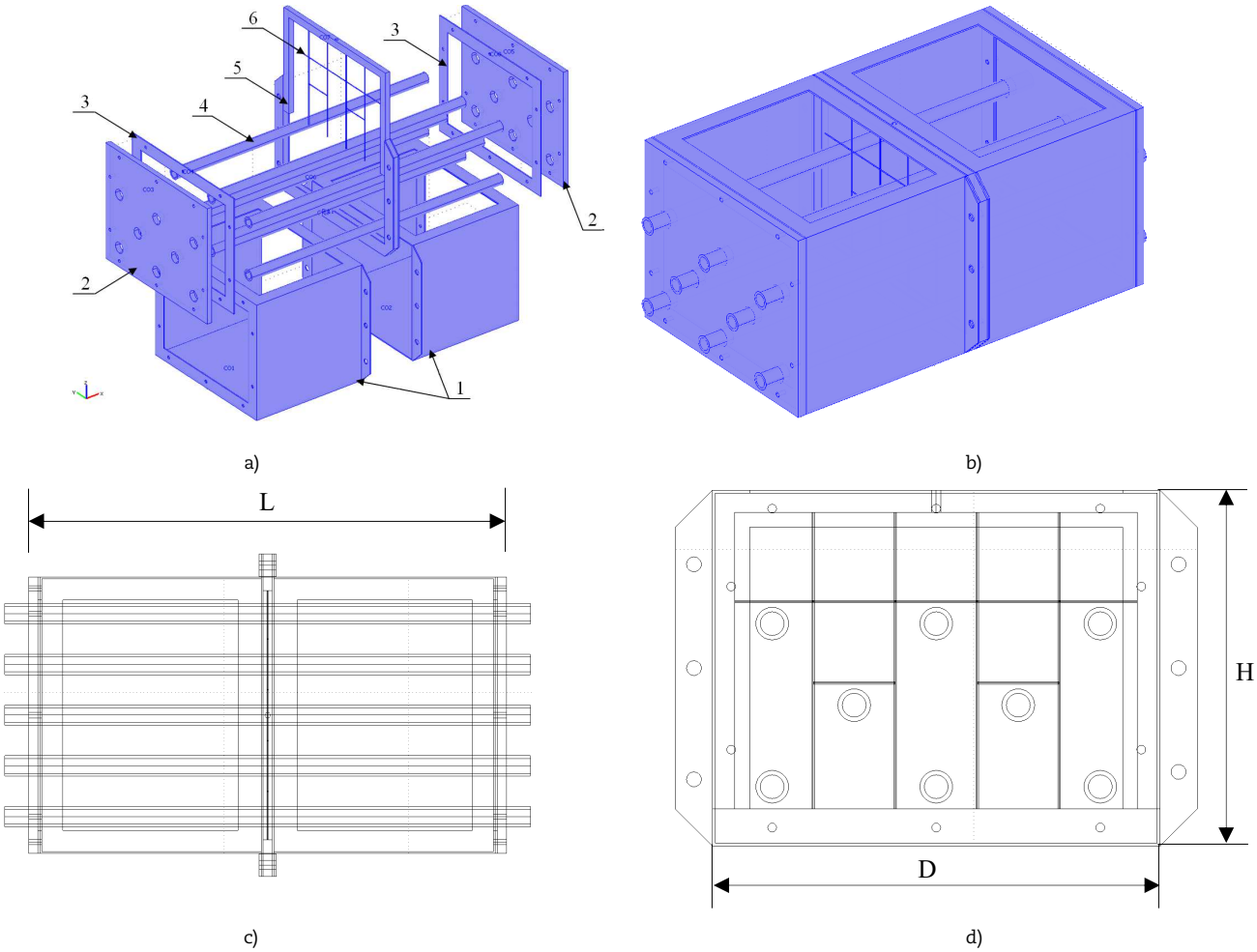

Fig. 1. The axonometric (a) and general (b) view of a heat accumulator model: 1 – a body; 2 – end covers; 3 - a sealing; 4 –a tube bundle; 5 – a slide; 6 – a sensor net

The mathematical model of the processes of heat and mass transfer at PCM phase transformations included Navier-Stokes equation and the equation of convective heat transfer [30-31].

$$\left.\begin{aligned}\frac{\partial \rho w_x}{\partial \tau}+w_x\frac{\partial \rho w_x}{\partial x}+w_y\frac{\partial \rho w_x}{\partial y}&=-\frac{\partial p}{\partial x}+\rho g_x+\frac{\partial}{\partial x}\left(\mu\frac{\partial w_x}{\partial x}\right)+\frac{\partial}{\partial y}\left(\mu\frac{\partial w_x}{\partial y}\right),\\ \frac{\partial \rho w_y}{\partial \tau}+w_x\frac{\partial \rho w_y}{\partial x}+w_y\frac{\partial \rho w_y}{\partial y}&=-\frac{\partial p}{\partial y}+\rho g_y+\frac{\partial}{\partial x}\left(\mu\frac{\partial w_y}{\partial x}\right)+\frac{\partial}{\partial y}\left(\mu\frac{\partial w_y}{\partial y}\right),\end{aligned}\right\} \tag{1}$$

$$\frac{\partial \rho}{\partial \tau}+\frac{\partial \rho w_x}{\partial x}+\frac{\partial \rho w_y}{\partial y}=0 \tag{2}$$

$$\frac{\partial T}{\partial \tau}+w_x\frac{\partial T}{\partial x}+w_y\frac{\partial T}{\partial y}=\frac{1}{\rho c_p}\frac{\partial}{\partial x}\left(\lambda\frac{\partial T}{\partial x}\right)+\frac{1}{\rho c_p}\frac{\partial}{\partial y}\left(\lambda\frac{\partial T}{\partial y}\right)\pm Q_s(x,y) \tag{3}$$

Initial and boundary conditions were of the following form:
- at the initial time point:

$$T(x,y,\tau=0)=T_0, \tag{4}$$

- on the body surface:

$$\left.\frac{dT}{dn}\right|_{s,c}=0, \tag{5}$$

- on the surface of cylindrical heat sources:

$$T_s(x,y)=T_{s,t} \tag{6}$$

When conducting numerical calculations of heat transfer in the area of accumulating material solid phase, the equation (3), which assumed that $w_x = 0$, $w_y = 0$ and where there were no convective heat-transfer parts, was applied.

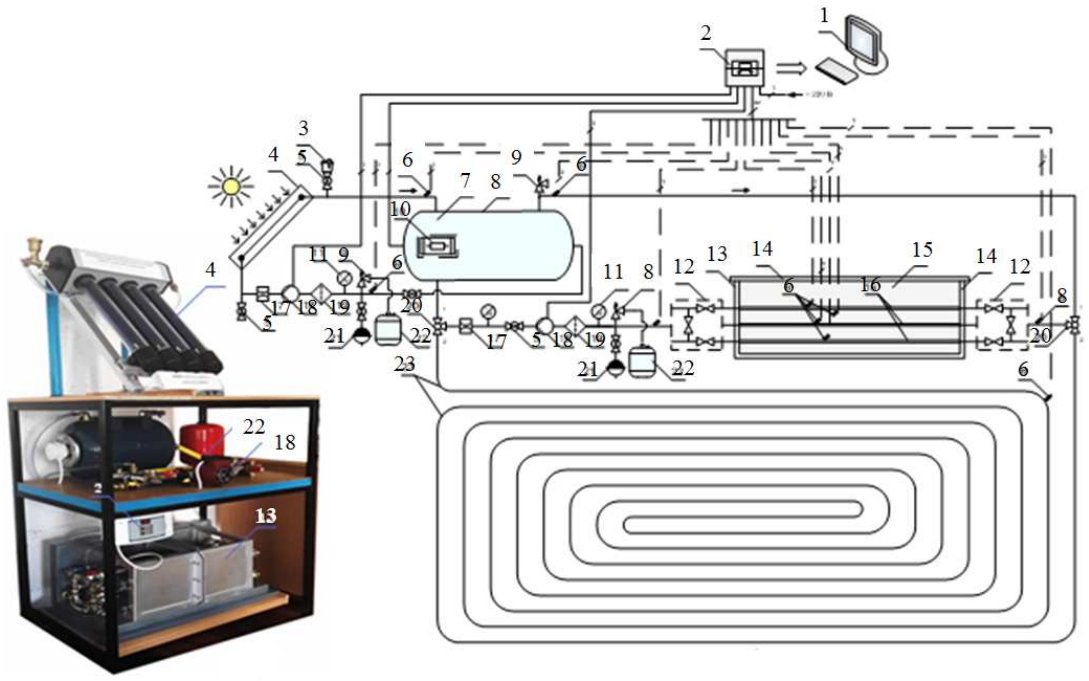

a) b)

Fig. 2. The overall view (a) and the hydraulic circuit (b) of the experimental plant: 1 – a computer; 2 – an analog-to-digital converter; 3 – an air bleed valve; 4 – a vacuum solar collector; 5 – a ball valve; 6 – a temperature sensor; 7 – a heat exchanger; 8 – an accumulator of a pressure tank; 9 – safety (discharge) valve; 10 – a back-up heat source (electric heating unit); 11 – a thermo-manometer; 12 – a distributing collector; 13 – an experimental module (heat accumulator); 14 – a heat sealing; 15 – an accumulating material; 16 – a tube bundle; 17 – a flow-rate meter; 18 – a circulating pump; 19 – a mesh filter; 20 – a three-way valve; 21 – an extension tank; 22 – a buffer tank; 23 – a "heat-insulated floor" heating system circuit.

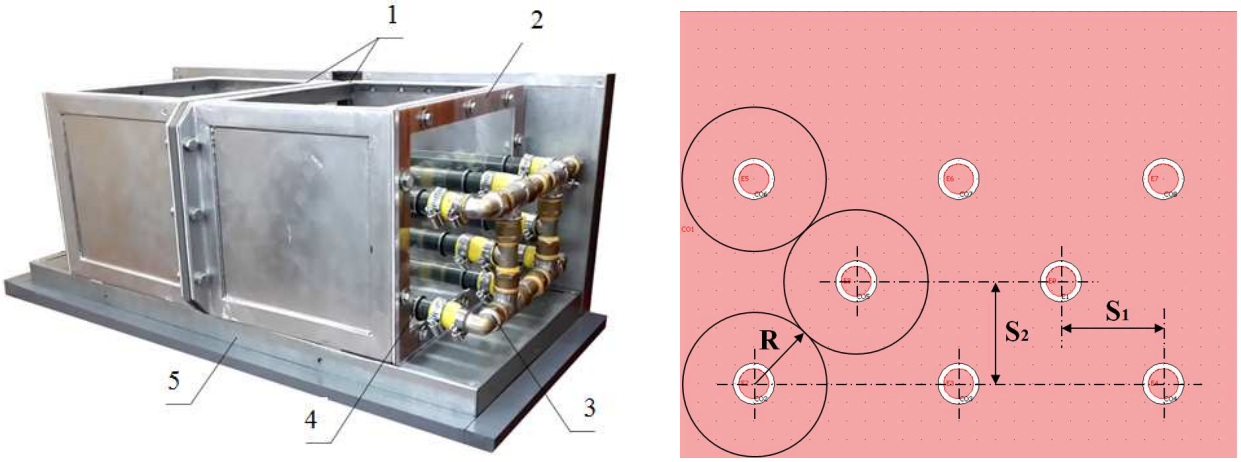

Fig. 3. The overall view of the experimental module (a) and the cross section of a tube bundle arrangement in a PCM volume (b): 1 – a sectionalized body; 2 – a face wall; 3 – a distributing collector; 4 – a tube bundle; 5 – a heat-insulating panel.

In order to verify the results of the conducted numerical investigation of the processes of heat and mass transfer during phase transformations of the accumulating material around several cylindrical heat sources, an experimental plant (Fig. 2) was developed. It consisted of a pressure tank used for water 8 applied with a back-up electric heating unit 10, a vacuum solar collector 4, which was a "charging" circuit of an experimental module of a heat accumulator 13, manometers 11, flow-rate meters 17 for determining heat carrier loss, a mesh strainer 19, shut-off valves and "heat-insulated floor" heating system 23 being 10 m^2, which was a "discharge" circuit cycle of the experimental module. All these elements were interconnected by pipelines and bypass lines, which made it possible to use various plant operation schemes. The system included automatic support and control of the main operating parameters (pressure and temperature) in installation diagrams, which was performed based on a digital USB-thermometer unit of MP707R series. The system provided heating or cooling of the accumulating material in the experimental module of a heat accumulator at maintaining the preset temperature of a heat carrier with further recording and visualization of the obtained results and parameter control on-line.

In order to test the veracity of the results of the conducted numerical modeling, an experimental module (Fig.3) was developed, made of steel and filled with solid material for heat accumulation. This module consisted of an oriented container (a body) in the form of a parallelepiped being H = 240 *mm* tall, L = 500 *mm* long and D = 300 *mm* wide. In order to provide even heat accumulation, a staggered tube bundle consisting of 8 steel tubes (d = 21.3 × 2.8 *mm*), arranged horizontally parallel to the bottom module wall with the equivalent radius around heat sources, which did not exceed R ≤ 40 mm (see Fig. 3b), according to the numerical modeling, was used. It was assumed that an apparatus operating time was equal to $\tau \approx 28800$ *s* (8 *hours*).

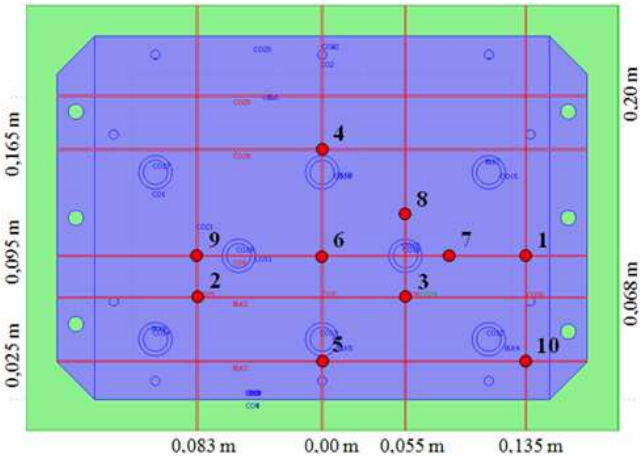

Fig. 4. The arrangement of temperature sensors on a "temperature mash" in a PCM volume (in the cross section relative to internal accumulator walls)

In order to measure temperature on the surface of cylindrical heat sources (a tube bundle) and in the volume of an accumulating material, digital temperature sensors were used. Temperature field control directly within a PCM volume was conducted with the help of 10 remote temperature sensors of Dallas DS18B20 type located in the so called "temperature mash" (Fig. 4), which was arranged inside the experimental module (at a distance of 250 *mm* from its end walls). The use of a "temperature mash" made it possible to monitor the dynamics of the temperature fields in the module under study. The measurement error, which was determined by the technical parameters of the equipment, was within the range of ± 0.5 °*C*.

The mass of an accumulating material (paraffin) in an operating camera was equal to M_{PCM} = 26.1 *kg*. Thermal-physical properties of an accumulating material were determined from the results of the laboratory tests and the properties of a heat carrier (water) based on the known tabulated values.

Such parameters as the temperature and the speed of a heat carrier were chosen to be the impact factors in the process of heat accumulation. As a parameter of heat accumulation process optimization, it was chosen to be the coefficient of material use efficiency, which was determined by the expression [32]:

$$\eta(\tau)=\frac{M_1(\tau)}{M_{PCM}}100\%\,, \tag{7}$$

where M_l and M_{PCM} – the mass of melted phase-change material and its total mass, respectively, *kg*; τ – a time span, *h*.

The indicated parameter showed the change in the mass of a melted material relative to the total PCM mass in various time points. The dynamics of this parameter change indicated the melting speed of a solid PCM, which is the main mechanism of heat accumulation in a heat accumulator.

Aimed at best representing the conditions of heat accumulation and extraction in an accumulating material, before the beginning of testing an operating camera was filled with melted paraffin and it was kept for the required period of time until its complete hardening and equalization of the temperature field in the whole paraffin volume $T_{нам}$ = const. Temperature indices were determined by temperature sensors in the module under study and in the environment (air). The initial conditions for conducting the experiments were considered to be met if the difference of these indices did not exceed 1 °*C*. Then a back-up thermo-electric heater (TEH) was turned on in a thermostat, which made it possible to maintain the temperature of a heat carrier at a constant level for every experimental set. In the process of conducting the investigations, there was temperature measurement performed on the surface of a tube bundle, measurement of heat carrier (water) temperature and the temperature in the paraffin volume conducted. The measurements were performed during 8 hours with the interval being Δτ =10 *m* during the first 120 minutes from the beginning of the experiment and with the interval being Δτ=30 *m* during the rest of the experimental period. At the end of the measuring process, total paraffin melting was provided, a "mesh" slide was moved at a distance of Δx = 10 *mm* and was fixed. Then, a cooling mode was maintained until complete paraffin hardening and total temperature equalizing in the whole volume. After the experimental measurements, the procedure of paraffin melting and "mesh" displacement was conducted again. After that the whole cycle of measurements was repeated.

The experimental investigations were conducted for several operation modes of an accumulator:

1) with gradual temperature increase of a heat carrier and PCM (the first set);
2) under the conditions of the maximum boundary heat carrier temperatures (the second set);
3) transition from heat accumulation ("charging") to heat extraction ("discharging") in a heat accumulator (the third set).

The test plan is presented in Table 1. When conducting the experiments at various modes, the experimental plant operation was performed under the pressure P_{hc}, produced by a circulation pipe with frequency regulation, which provided a smooth change of a heat carrier costs within the range of G_{hc}=1.5–2.5 *l/m* for every set of the experiments.

The investigations concerning the first set were performed at simultaneous engaging of a pipe and a water heater. Here, the temperature of a heat carrier (water) was changed within the limits of t_{wat}=55÷80 °*C*. The second and the third set of the experiments was conducted with prior heating of the water in a tank to the temperature of t_{wat}=80 °C. Then, the pumping of a heat carrier through the module was performed. The third set was different from the second one by synchronous TEH turning off at a given time and a switch of pipe operation mode to heat carrier circulation around a loop: a "heat-insulated floor" heating system - the module under study. Such a mode is typical for accumulator operation in a "discharge" mode. Here, the temperature of a heat carrier in the system was maintained within the limits of t_{wat}=45÷35 °*C*. Before the beginning of the experiment, a computer was switched on and the recording of the measurement results was conducted at the set pitch of temperature recording.

Table 1. Test plan

t_{wat} (°C)	Margin of fluctuations t_{wat} (°C)	G_{cm} (*l*/*m*)	P_{hc} (*bar*)	Margin of fluctuations P_{hc} (*bar*)	Set
+55	55 ÷ 56	2.0	1.1	1.0 ÷ 1.2	№ 1
+61	60 ÷ 62				
+65	64 ÷ 66		1.2	1.1 ÷ 1.3	
+70	69 ÷ 72				
+75	73 ÷ 76	1.5	1.6	1.5 ÷ 1.7	
		2.0	1.3	1.2 ÷ 1.4	
		2.5	1.1	1.0 ÷ 1.2	
+80	78 ÷ 82	1.5	1.8	1.7 ÷ 1.9	
		2.0	1.5	1.4 ÷ 1.6	
		2.5	1.4	1.3 ÷ 1.5	
+81	80 ÷ 82	1.5	1.8	1.7 ÷ 1.9	№ 2
		2.0	1.5	1.4 ÷ 1.6	
		2.5	1.4	1.3 ÷ 1.5	
+40	35 ÷ 45	2.5	1.5	1.4 ÷ 1.6	№ 3

3. Results and Discussion

As a result of the conducted numerical modeling (Fig. 5) and the experimental investigations, temperature field distributions in a PCM volume has been obtained (Fig.5) as well as the change in the profile of melting boundaries (Fig. 6) around cylindrical sources has been determined at various time points.

Fig. 7 presents experimentally determined graphical dependences of volume-averaged temperature values on the time spent in melted and unmelted PCM mass at various inlet temperature values of a heat carrier.

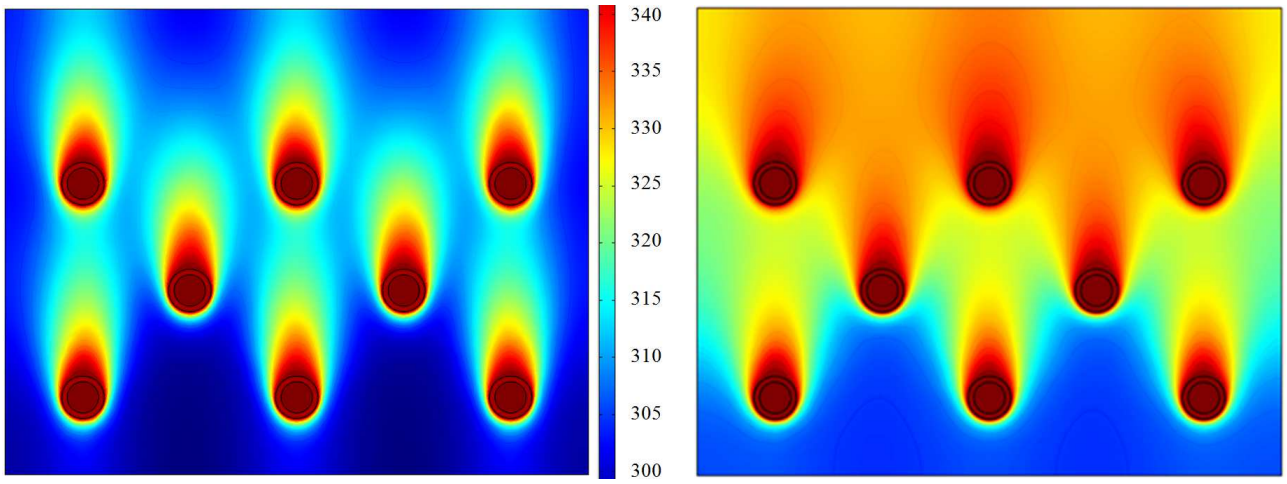

Fig. 5. Temperature fields in PCM cross section for a heat accumulator at various time moments: a, c – 30 min; b, d – 180 min.

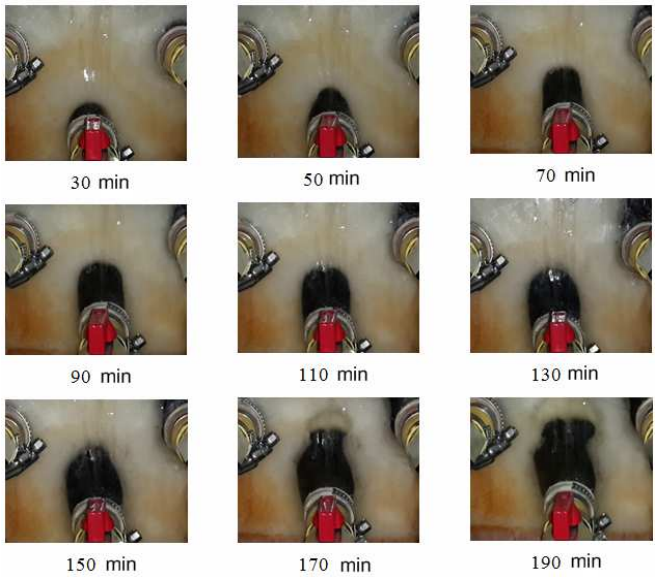

Fig. 6. Melting profile change in the system "solid body-melt" within the range of time moments being 0-190 min

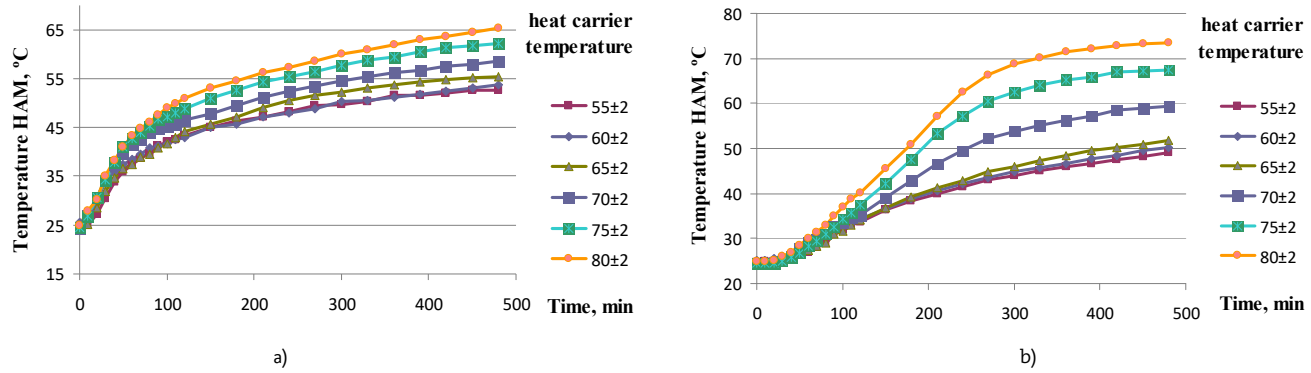

Fig. 7. Temperature change in the volume of an accumulating material at various inlet temperature values of a heat carrier: a – in "stagnant areas"; b – in material melt.

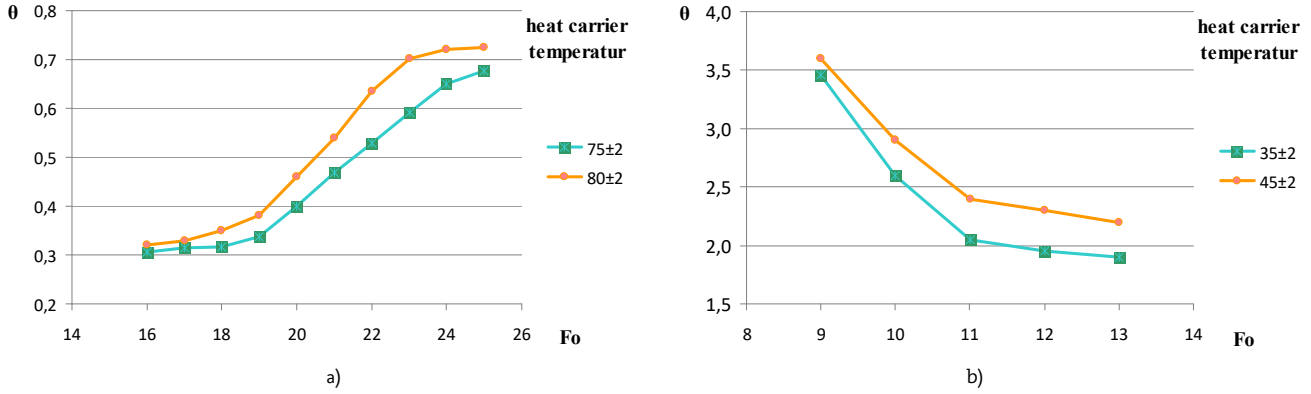

Fig. 8. Average bulk temperature θ-vs-Fourier's number Fo dependence during melting (a) and crystallization (b) of an accumulating material

The conducted numerical modeling has made it possible to obtain the dynamics of the change in the average PCM bulk temperatures in time. Fig. 8 presents the dependence of the non-dimensional temperature $\theta = (\overline{T} - T_{ext}) / (T_f - T_{ext})$ on Fourier's number Fo = λ_{tsm} τ/(d/2) 2 for liquid and solid PCM phases at heat accumulator "charging" and "discharging" ($\overline{T}$ - the average temperature of a phase-change material, T_f – melting temperature of a phase-change material, T_{xt} – environment temperature, λ_{PCM} – the coefficient of PCM heat conductivity).

Having analyzed the results of the numerical modeling, it has been possible to determine three phases of heat accumulation in PCM . At the first phase the main mechanism of heat transfer is a conductive heat transfer in a solid PCM . Here, a thin sheet of melt is created around a cylindrical heat source and the influence of convection on the processes of heat transfer is insignificant. At the second phase of heat accumulation, convective heat transfer followed by an intensive accumulating material melting is a dominating one. Here, the temperature in a melted PCM is close to the temperature of PCM melting and does not change significantly over time. The third phase begins when PCM , which is located above a tube bundle, is completely melted. This stage is characterized by overheating of a melted material mass and slow melting of a solid mass of the material arranged in the lower part of a heat accumulator.

The conducted investigations have shown that the maximum speed of heat accumulation and the increase of the coefficient of material use efficiency η(τ) is typical for the second melting phase. Here, the greatest melted material mass increase per time unit has been observed. In case of the third phase, a great amount of heat is spent on overheating the volume of a melted mass, which temperature exceeds the temperature of an unmelted PCM mass located in the lower part of an accumulator ("stagnant areas") for 10-12% (Fig. 6). This phase is characterized by a low increment of the coefficient of material use efficiency and η(τ) the minimum value of the accumulated heat per PCM mass in unit time. The duration of this phase is equal to approximately 25% of the total time of heat accumulation, when an accumulator is in its "charge" mode.

The value of the coefficient of material use efficient (see Equation (7)) has been within the limits of 0.55÷0.74 depending on the inlet heat carrier temperature and heat accumulator operation modes.

One of the important characteristics of a heat accumulator is the speed of heat accumulation per PCM mass unit, which depends on the inlet heat carrier temperature and the geometry of heat sources arrangement in the volume of an accumulator. The numerical calculations of the processes of PCM melting at various values of an outer diameter, longitudinal and transverse pitches of cylindrical heat sources S1, S2 arranged in a staggered tube bundle as well as at a distance from side and bottom body walls, have been conducted (see Fig. 3b). As a result of the conducted numerical calculations, it has been determined that the speed of heat accumulation in a PCM mass unit is the maximum one at certain values of the equivalent radius R between heat sources, the walls and the bottom of an accumulator (see Fig. 3b). The results of the conducted calculations of radius R values for various tube diameters are presented in Table 2.

Having analyzed the results of the conducted numerical modeling, it has been determined that the distance of the lower and the side rows of heating elements from the bottom and the side walls of an accumulator body should not exceed the values of the radius R, which are shown in Table 1.

The conducted experimental investigations have verified the results of the numerical modeling. The choice of the optimum distance between cylindrical heat sources and the bottom body wall results in the decrease of stagnant areas during heat energy accumulation and the cutting of heat accumulator "charging" time for 15-20%.

Table 2. Values of the optimal distance (radius) between heat sources, the bottom and the side walls in accumulating material volume depending on the diameter of cylindrical sources.

Parameter	Nominal diameter (*inches*)					
	½	¾	1	1 ¼	1 ½	2
External diameter of tubes (*mm*)	21.25	26.75	33.50	42.25	48.00	60.00
Optimal radius R (*mm*)	30.00	35.00	45.00	57.00	70.00	85.00

The comparison of the numerical modeling results (curves 1, 3, Fig. 9) and the experimental data (curves 2, 4) for the processes of melting (curves 1, 2, Fig. 9 – accumulator "charge") and crystallization (curves 3, 4, Fig. 9 – accumulator "discharge") has been conducted. The difference between the numerical and the experimental data for the volume-averaged PCM temperatures during melting (curves 1 and 2, Fig.9) does not exceed 3%, and during its crystallization it is less than 5% (curves 3 and 4, Fig. 9).

Taking into account the presence of "stagnant areas" during PCM melting in the lower part of the material volume, which is located near the bottom of an accumulator body, the advanced design of a body, which decreases the presence of such areas, has been suggested (Fig. 10a). In this heat accumulator design the surface of the bottom wall has a wave form with the radius of curvature being R_b for a curvilinear surface element, which is then duplicated (see Fig 10a).

The numerical modeling of the processes of melting in the heat accumulator of a new design has been conducted. Fig. 9b presents the distribution of the temperature fields in the cross section of a heat accumulator. The comparison of these distributions for a heat accumulator, which has a cross section of a rectangular form (see Fig. 4b) and the accumulator of the improved design (Fig. 10b) has shown the absence of stagnant areas with worse heat transfer conditions in the suggested heat accumulator design. Here, in the process of heat accumulator "charging", there is even phase-change material melting in the whole accumulator volume. It has made it possible to cut the time required for the complete phase-change material melting for 12-15% and improve the efficiency of a heat accumulator.

The conducted analysis (Table 3) has shown that the accumulator of a new design has the improved increment dynamics of the coefficient of material use efficiency $\eta(\tau)$, the increase of a melted TAM mass $M_{l2} > M_{l1}$ per time unit and the improved accumulator effectiveness.

The analysis of Table 3 data has shown that the use of a waveform body bottom of the apparatus can provide a 26 % increase of the coefficient of material use efficiency at the same weight-size parameters of both accumulators.

The results of numerical and experimental studies of heat accumulation (selection) in heat accumulators with phase transformations of PCM (paraffin) and the improved design of the heat accumulator can be used for heat accumulation from renewable energy sources such as solar collectors, heat pumps and other sources. This is due to the low melting point of PCM, which is 54 ÷ 56 °C, high density of heat accumulation per unit mass of PCM and minimization of areas where the rate of heat accumulation (selection) is significantly less than in the main volume of PCM.

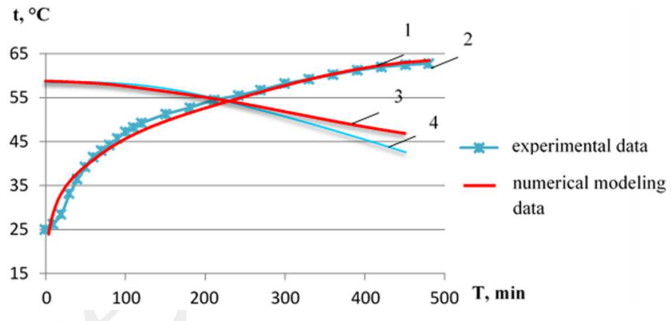

Fig. 9. Comparison of the numerical modeling results (1, 3) and the experimental data (2, 4) on the temperature characteristics of a phase-change material in the process of heat accumulator "charging" and "discharging"

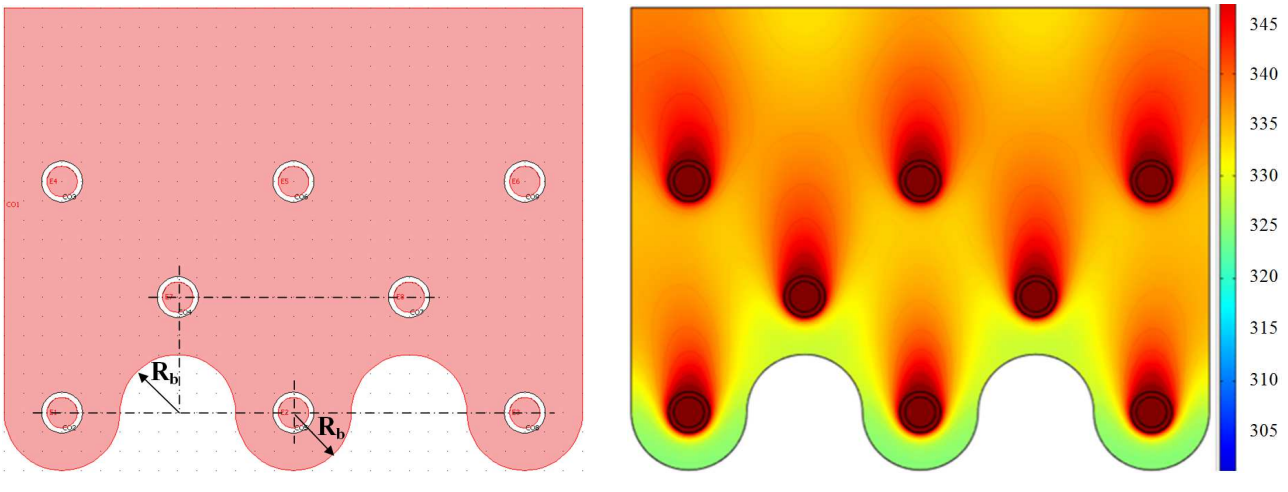

a) b)

Fig. 10. Overall view of the cross section of the heat accumulator of a new design (a) and the distribution of temperature fields in this cross section (b)

Table 3. Results of the comparative analysis of a heat accumulator with phase transformations of the design under study and the improved design

Operation time (h)	Previous design	Improved design
	Coefficient of material use efficiency (η)	
0	0.000	0.000
1	0.024	0.041
2	0.090	0.131
3	0.124	0.179
4	0.173	0.255
5	0.279	0.366
6	0.407	0.497
7	0.552	0.738
8	0.736	1.000

4. Conclusion

1. The numerical modeling and the experimental investigations of the processes of heat and mass transfer at phase transformations of an accumulating material around a staggered tube bundle of cylindrical heat sources has been conducted applying COMSOL Multiphysics 3.5a software and three heat accumulation phases have been determined. The main mechanism of heat accumulation has been determined to be a convective heat transfer at an intensive phase-change material melting, which is typical for the second phase of heat accumulation.

2. It has been determined that there are "stagnant areas" in the bottom part of a heat accumulator, which results in the deceleration of melting processes and the decrease in the coefficient of material use efficiency of phase-change material mass, which characterizes the speed of heat accumulation in an accumulator.

3. As a result of the conducted numerical calculations, the optimal distance (radius) R between cylindrical heat sources, bottom and side accumulator walls, at which the value of "stagnant areas" is decreased and accumulator heat-accumulating capacity is increased, has been determined.

4. A new design of a heat accumulator has been suggested. It minimizes the presence of "stagnant areas" and improves the effectiveness of accumulator performance. The use of the new accumulator design has made it possible to shorten the time required for complete PCM melting and increase its efficiency compared to the known identical devices.

Author Contributions

The authors I. Antipov and V. Gorobets proposed a new construction of heat accumulator. I. Antipov and V. Trokhanyak performed experimental research and numerical modeling of mass and heat transfer processes during phase transformations of PCM. V. Gorobets and I. Antipov conducted an analysis and revealed the basic laws of thermal energy accumulation processes in batteries with phase transformation of PCM.

Conflict of Interest

The authors declared no potential conflicts of interest with respect to the research, authorship and publication of this article.

Funding

Publication is based on the research provided by the grant support of the State Fund for Fundamental Research of Ukraine, the Ministry of Education and Science of Ukraine (project No F64/11-2016).

Nomenclature

λ	Heat conductivity coefficient [W/(m•K)]	Q	Heat source capacity [W]
μ	Coefficient of kinematic viscosity [Pa•s]	R	Equivalent radius [mm]
ρ	Density [kg/m3]	T	Temperature [K]
τ	Time [s]	t	Temperature [°C]
η	Coefficient of material use efficiency	s	Surface [m^2]
d	Tube diameter [mm]	w	Speed [m/s]
G	Consumption of a heat carrier	x, y, z	Cartesian coordinates [m]
n	Normal to the surface of the body	f	Melting
p	Pressure [Pa]	l	Melt
H	Accumulator height [mm]	PCM	Phase-change materials
L	Accumulator length [mm]	0	Reference time
W	Accumulator width [mm]	wat	Water
M	Mass [kg]	ext	Environment

References

[1] Sharma, A., Tyagi, V., Chen, R., Buddhi, D., Review on thermal energy storage with phase-change materials and applications, *Renewable and Sustainable Energy Reviews*, 13(2), 2009, 318–345.

[2] Du, K., Calautit, J., Wang, Z., Wu, Y. & Liu, H., A review of the applications of phase change materials in cooling, heating and power generation in different temperature ranges, *Applied Energy*, 220, 2018, 242–273.

[4] Pereira, da Cunha, J., Eames, P., Thermal energy storage for low and medium temperature applications using phase change materials – A review, *Applied Energy*, 177, 2016, 227–238.

[4] Kenisarin, M. M., Thermophysical properties of some organic phase change materials for latent heat storage. A review, *Solar Energy*, 107, 2014, 553–575.

[5] Fan, L., Khodadadi, J., Thermal conductivity enhancement of phase change materials for thermal energy storage: A review, *Renewable and Sustainable Energy Reviews*, 15(1), 2011, 24–46.
[6] Suganya, G., Ramesh-Bapu, B., Experimental studies on performance of latent heat thermal energy storage unit integrated with solar water heater, *Engineering International Journal of Chemical Sciences*, 14(2), 2016, 1165–1171.
[7] Agyenim, F., Hewitt, N., Eames, P., Smyth, M., A review of materials, heat transfer and phase change problem formulation for latent heat thermal energy storage systems (LHTESS), *Renewable and Sustainable Energy Reviews*, 14(2), 2010, 615–628.
[8] Kalaiselvam, S., Veerappan, M., Arul, A., Iniyan, S., Experimental and analytical investigation of solidification and melting characteristics of PCMs inside cylindrical encapsulation, *International Journal of Thermal Sciences*, 47(7), 2008, 858–874.
[9] Sharma, R. K., Ganesan, P., Tyagi, V. V., Metselaar, H. S. C., Sandaran, S. C., Developments in organic solid–liquid phase change materials and their applications in thermal energy storage, *Energy Conversation and Management*, 95, 2015, 193–228.
[10] Trivedi, G. V. N., Parameshwaran R., Cryogenic conditioning of microencapsulated phase change material for thermal energy storage, *Scientific Reports*, 10, 2020, 18353.
[11] Huo, Y., Rao, Z., Lattice Boltzmann simulation for solid–liquid phase change phenomenon of phase change material under constant heat flux, *International Journal of Heat and Mass Transfer*, 86, 2015, 197–206.
[12] Wang, F., Lin, W., Ling, Z., Fang, X., A comprehensive review on phase change material emulsions: Fabrication, characteristics, and heat transfer performance, *Solar Energy Materials and Solar Cells*, 191, 2019,218–234.
[13] Lichołai, L., Musiał, M., Experimental Analysis of the Function of a Window with a Phase Change Heat Accumulator, *Materials*, 13(16), 2020, 3647.
[14] Liu, L., Su, D., Tang, Y., Fang, G., Thermal conductivity enhancement of phase change materials for thermal energy storage: A review, *Renewable and Sustainable Energy Reviews*, 62, 2016, 305-317.
[15] Regin, A., Solanki, S., Saini, J., Latent heat thermal energy storage using cylindrical capsule: numerical and experimental investigations, *Renewable Energy*, 31, 2006, 2025–2041.
[16] Zhang, Q., Huo, Y., Rao, Z., Numerical study on solid–liquid phase change in paraffin as phase change material for battery thermal management, *Science Bulletin*, 61(5), 2016, 391–400.
[17] Jegadheeswaran, S., Pohekar, D., Performance enhancement in latent heat thermal storage system: A review, *Renewable and Sustainable Energy Reviews*, 13(9), 2009, 2225–2244.
[18] Gorobets, V., Treputnev, V., Heat transfer and the motion of the interphase boundary, when a PCMis melted near a horizontal heat source with section finning, *Teplofizika Vysokikh Temperatur*, 33(4), 1995, 588–593.
[19] Arshad, A., Ali, H. M., Ali, M., Manzoor, S., Thermal performance of phase change material (PCM) based pin-finned heat sinks for electronics devices: Effect of pin thickness and PCM volume fraction, *Applied Thermal Engineering*, 112, 2017, 143–155.
[20] Kuboth ,S., König-Haagen, A., Brüggemann, D., Numerical Analysis of Shell-and-Tube Type Latent Thermal Energy Storage Performance with Different Arrangements of Circular Fins, *Energies*, 10, 2017, 274.
[21] Mohamad, A.A., *Lattice Boltzmann Method: Fundamentals and Engineering Applications with Computer Codes*, Springer-Verlag, London, 2019.
[22] Karimnejad, S., Amiri Delouei, A., Nazari, M., Shahmardan, M.M., Rashidi, M.M., Wongwises, S., Immersed boundary-thermal lattice Boltzmann method for the moving simulation of non-isothermal elliptical particles, *Journal of Thermal Analysis and Calorimetry*, 138(6), 2019, 4003-4017.
[23] Gorobets, V., Antypov, I., Bohdan, Y., Trokhaniak, V., Numerical and experimental researches of thermal energy storage processes during phase transformations of phase change materials with nanoparticles, *E3S Web of Conferences*, 128, 2019, 04003.
[24] Nasieka, Iu., Strelchuk, V., Naseka, V., Stubrov, Yu., Dudnik, S., Gritsina, V., Opalev, O., Koshevoy, K., Strel'nitskij, V., Tkach, V., Boyko, M., Antypov, I., An analysis of the specificity of defects embedded into (100) and (111) faceted CVD diamond microcrystals grown on Si and Mo substrates by using E/H field discharge, *Journal of Crystal Growth*, 491, 2018, 103–110.
[25] Trp, A., An experimental and numerical investigation of heat transfer during technical grade paraffin melting and solidification in a shell-and-tube latent thermal energy storage unit, *Solar Energy*, 79, 2005, 648–660.
[26] Naumov, A.L., Serov, S.F., Efremov, V.V., Degtyarev, N.S., *RU Patent No. 2436020*, 2011.
[27] Gorobets, V., Antypov, I., Trokhaniak, V., Bohdan, Y., Experimental and numerical studies of heat and mass transfer in low-temperature heat accumulator with phase transformations of accumulating material, *MATEC Web of Conferences*, 240, 2018, 01009.
[28] Chen, S.L., Hsiao, M.J., *US Patent No. 6220337*, 2001.
[29] Al Hallaj, S., Selman, J.R., *US Patent No. 6468689*, 2011.
[30] Khmelnik, S.I., Navier-Stokes equations. On the existence and the search method for global solutions, *Mathematics in Computers*, Bene-Ayish, 2018.
[31] Gorobets, V.G., Bohdan, Yu.O., Trokhaniak, V.I., Antypov, I.O., Experimental studies and numerical modelling of heat and mass transfer process in shell-and-tube heat exchangers with compact arrangements of tube bundles, *MATEC Web of Conferences*, 240, 2018, 02006.
[32] Kukolev, M.I., Fundamentals of designing heat energy accumulators, *Petrozavodsk: PetrHU*, Russia, 2001.

ORCID iD

Ievgen Antypov https://orcid.org/0000-0003-0509-4109
Valery Gorobets https://orcid.org/0000-0003-1180-4509
Viktor Trokhaniak https://orcid.org/0000-0002-8084-1568

How to cite this article: Antypov I., Gorobets V., Trokhaniak V. Experimental and numerical investigation of heat and mass transfer processes for determining the optimal design of an accumulator with phase transformations, *J. Appl. Comput. Mech.*, 7(2), 2021, 611–620. https://doi.org/10.22055/JACM.2020.34893.2524